Cisplatin tethered gold nanoparticles which exhibit enhanced reproducibility, drug loading and stability – a step closer to pharmaceutical approval?

Gemma E. Craig,[1] Sarah D. Brown,[1] Dimitrios A. Lamprou,[1] Duncan Graham[2] and Nial J. Wheate[1,3]*

[1]Strathclyde Institute of Pharmacy
and Biomedical Sciences,
Arbuthnott Building,
University of Strathclyde,
161 Cathedral Street,
Glasgow, G4 0RE,
United Kingdom.

[2]Centre for Molecular Nanometrology,
Department of Pure and Applied Chemistry,
Thomas Graham Building,
University of Strathclyde,
295 Cathedral Street,
Glasgow, G1 1XL,
United Kingdom.

[3]Faculty of Pharmacy,
The University of Sydney,
NSW, 2171, Australia.

* nial.wheate@sydney.edu.au; fax: + 61 2 9351 4391

Abstract

Gold nanoparticles (AuNPs) can be used as delivery vehicles for platinum anticancer drugs, improving their targeting and uptake into cells. Here, we examine the appropriateness of different sized AuNPs as components of platinum based drug-delivery systems, investigating their controlled synthesis, reproducibility, consistency of drug loading and stability. The active component of cisplatin was tethered to 25, 55 and 90 nm AuNPs; with the nanoparticles being almost spherical in nature and demonstrating good batch-to-batch reproducibility (24.37 ± 0.62 nm, 55.2 ± 1.75 nm and 89.1 ± 2.32 nm). The size distribution of 25 nm AuNPs has been significantly improved, compared with a previous method which produces polydispersed nanoparticles. Attachment of platinum to the AuNP surface through a polyethylene glycol (PEG) linker exhibits an increase in drug loading with increasing particle size: 25 nm (815 ± 106 drug molecules per AuNP); 55 nm (14,216 ± 880); and 90 nm (54,487 ± 15,996). The stability of the naked, PEGylated and platinum conjugated nanoparticles has been examined over time under various conditions. When stored at 4 ºC there is minimal variation in diameter for all three AuNP sizes; variation after 28 days for the 25 nm AuNPs was 2.4%; 55 nm, 3.3%; and 90 nm, 3.6%. The 25 nm AuNPs also demonstrate minimal changes in UV-visible absorbance over the same time period.

Introduction

Cisplatin, *cis*-diamminedichloridoplatinum(II), is the leading metallodrug used in the systemic treatment of solid tumors.[1] Its clinical use is limited by severe toxic side effects, attributed to the indiscriminate accumulation of the drug in both normal and cancerous tissue, its non-specific interactions with extra- and intracellular proteins, and drug resistance, both intrinsic and acquired.[2] The focus of drug development is now being directed towards delivery vehicles which can overcome these limitations, and can specifically target cancerous cells.

Due to the unique disorganised vasculature of cancer cells with numerous pores, coupled with compromised lymphatic drainage, nanoparticles can passively target solid tumours, leading to an enhanced permeability and retention (EPR) effect.[3] This EPR effect can be utilised by nanotechnology-based drug delivery as it enhances the accumulation of the drug in tumours and minimises uptake by healthy cells.[4] For optimal efficacy, nanoparticle-based systems must take into consideration the gaps in the tumour vasculature endothelium, which can range from 100 nm to 2 μm,[5] and nanoparticle clearance, which varies with nanoparticle size.[6]

Gold nanoparticles (AuNPs) are particularly attractive as chemotherapy delivery vehicles as they are non-toxic, biocompatible and easily synthesised.[7-12] In addition to size, their cellular uptake is dependent upon shape and surface charge.[13-15] There are two important considerations in the endocytosis of gold nanoparticles; the binding energy between the ligand and receptor, and the free energy required to drive the nanoparticles into the cell.[13] Uptake is limited for either extremely small or large nanoparticles, with the optimal diameter reported as between 40-60 nm.[6, 13-15]

We have previously shown that tethering the active component of the platinum anticancer drug oxaliplatin to a 20 nm gold nanoparticle via a thiolated PEG linker increases cytotoxicity, compared with oxaliplatin alone, and demonstrates nuclear penetration.[16] Gold nanoparticles and gold nanorods have also been used as platforms for the delivery of platinum(IV) prodrugs, demonstrating enhanced cellular uptake and superior cytotoxicity compared with cisplatin.[17, 18] Cisplatin has been loaded onto gold nanoparticles of the form Au-Au_2S and Au-Fe_3O_4 for photodynamic thermal therapy and magnetically controlled delivery, respectively.[19, 20]

Demonstrating that drugs can be tethered to nanoparticles, and that these conjugates improve drug uptake and/or activity, is just the first step in the long and complex drug approval process. There are a number of other crucial factors to consider which, to our knowledge, for this type of platinum based drug-delivery vehicle have yet to be investigated. Constructing a drug-nanoparticle conjugate with reproducible size and shape which demonstrates consistent drug loading, is important for its ability to be administered for therapeutic use; i.e., it ensures the concentration of delivered drug remains constant. Stability, both during manufacture and storage, must also be established to guarantee that the performance is unaffected and the system remains safe.

In this paper we report the construction of platinum tethered gold nanoparticle conjugates using the active component of the common anticancer drug cisplatin (Figure 1). This has been achieved for small, medium and large AuNPs (25, 55 and 90 nm, respectively), where the synthesis shows good reproducibility and monodispersity. The drug-nanoparticle conjugates have been characterised using UV-visible spectrometry, dynamic light scattering (DLS), and atomic force microscopy (AFM). The platinum drug was tethered to the AuNPs using a polyethylene glycol (PEG) linker, and drug loading was determined using inductively coupled plasma-

mass spectrometry (ICP-MS). Finally, we have determined the effect of platinum drug concentration on the stability of the AuNPs during synthesis, as well as examining the growth of naked, PEGylated and drug conjugated nanoparticles under various conditions.

Results and Discussion

Construction of drug-nanoparticle conjugate

The size of a gold nanoparticle can be controlled via the route of synthesis; the Brust-Schiffrin synthesis involves an organic two-phase reduction and typically yields AuNPs 5-6 nm in diameter.[21] The Turkevich-Frens method of reducing a gold salt with sodium citrate has been reported to produce nanoparticles of 9-120 nm,[22] with larger nanoparticles in the region of 50-200 nm being produced via the reduction of $HAuCl_4$ with hydroquinone in an aqueous solution containing seeds.[23] Our aim was to synthesise small, medium and large AuNPs (25, 55 and 90 nm, respectively) which demonstrate good reproducibility. This is a necessity in the construction of a drug-delivery vehicle to ensure a consistent drug payload is being administered and that the response, whether in vitro or in vivo, can be accurately predicted.

The nanoparticles synthesised in this study have been produced from the reduction of sodium tetrachloroaurate(III) by tribasic sodium citrate, where the size of the nanoparticles is determined primarily by the pH of the solution, which in turn is controlled by the concentration of sodium citrate.[24] In this method sodium citrate functions as both the nucleating and growth agent,[7] as well as distributing a negative charge on the nanoparticle surface to minimise aggregation. A higher citrate concentration allows for the stabilisation of smaller particles, while at lower

concentrations, the coverage is incomplete and a coarsening process leads to aggregation, producing larger particles.[22] These larger nanoparticles have been shown to sometimes be polydispersed and yield low particle concentrations.[25]

Nanoparticles, 25 nm in diameter, were initially synthesised via the established citrate reduction method.[7, 26] This, however, produced a bimodal size distribution curve, as determined by dynamic light scattering (DLS), with peaks at 3.4 and 45.4 nm (Figure 2). This is problematic as it is only with monodispersed systems that a reliable and precise dosage of drugs can be assured. A reactant concentration study, where we varied the volume of citrate solution, led to the development of a new method for synthesising 25 nm AuNPs demonstrating monodispersity (Figure 2) and better reproducibility (Table 1). For both the old method (Turkevich-Frens) and our revised method, the concentration (% w/v) of the gold salt and citrate solutions remain the same, however, using a 2.7-fold increase in the volume of citrate solution, we reproducibly synthesise spherical, monodispersed 25 nm AuNPs.

Table 1. The reproducibility of 25 nm AuNPs produced by the two synthetic methods, where the mean hydrodynamic diameter (z-avg.) and the highest peak from the intensity particle size distribution curve (i.e. the relative percentage of light scattered by particles of different diameters) were determined by DLS. Results from three batches of AuNPs demonstrate the improved size reproducibility of our revised method.

Method	***Average Particle Diameter (nm)***	***Highest Intensity Peak (nm)***
Turkevich-Frens	17.9 ± 4.1	46.6 ± 4.9
Revised	22.9 ± 0.6	24.4 ± 0.6

Methods to synthesise 55 and 90 nm gold were also developed and, as expected, lower concentrations of citrate were required to produce nanoparticles of these sizes. Larger AuNP synthesis method displayed good reproducibility, as observed across five batches of AuNPs where small size variations (55.2 ± 1.75 nm and 89.1 ± 2.32 nm) were observed. In addition, both the 55 and 90 nm AuNPs were found to show improved size uniformity compared with previous synthesis methods.[26, 27] In synthesising the larger AuNPs, it was noted that when the gold salt was not stored in a desiccator, there was significant variation in the size of the nanoparticles produced. This effect was also observed when water loss from the reaction vessel was not minimised, hence affecting the reactant concentration and altering the size of the AuNPs produced. Therefore, when synthesising 55 and 90 nm AuNPs, it is important to use an anhydrous gold salt and control water loss through evaporation.

Attachment of the active component of cisplatin, cis-$\{Pt(NH_3)\}^{2+}$, to the AuNPs is facilitated through a polyethylene glycol (PEG) monolayer. PEG-based linkers are extensively used in the functionalisation of AuNPs as they are stable, non-toxic, reduce non-specific binding to proteins and possess good water solubility.[28] A large number of PEG linkers can be accommodated due to the high surface area of gold nanoparticles,[29, 30] and in addition to improving stability, circulation time, and cellular uptake, they provide an attachment site for drugs and/or cancer targeting groups.[28-31] It has been shown that linkers with multi-thiol anchors, compared with their monothiol analogues, show enhanced stability when treated with small molecule reducing/displacement agents such as dithiothreitol (DTT).[31] PEGylation of the AuNPs in this study was accomplished by agitating the linker with nanoparticles at appropriate concentrations, as determined by UV-visible spectroscopy and size-dependent extinction coefficients, overnight. Experimental parameters for each size of gold nanoparticle are given (Table 2).

Table 2. Experimental parameters for the PEGylation and purification of the three different sized AuNPs.

Size of AuNP (nm)	Concentration of AuNP to be PEGylated (nM)	Extinction coefficient,[32] (ε, $M^{-1}cm^{-1}$)	Centrifuge settings	
			Speed (RPM)	Time (min)
25	17	2.7×10^8	7000	20
55	0.17	2.65×10^{10}		7
90	0.017	1.346×10^{11}		2

The final stage in the assembly of the drug-nanoparticle conjugates was the coupling of the platinum drug to the PEGylated AuNPs. To facilitate this, cisplatin was first aquated to replace the chloride ligands with the more labile leaving group, water. The concentration of drug used in this step was directly adapted from our previous study,[16] however, for many early batches we found that the nanoparticles turned a blue-purple colour upon addition of platinum, measured as a red of λ_{max} of the AuNPs or shoulders/additional peaks in the UV-visible spectra (supplementary information). This is indicative of AuNP aggregation,[33] and in some cases aggregates precipitated out of solution and could not be resuspended. We believe this is a result of the decreased surface charge on the nanoparticles as they go from negatively charged (from the carboxylate groups on the PEG linker) to neutral. To eliminate this problem and determine maximum platinum loading, concentration studies were performed for each of the three different sized nanoparticles, using zeta potential as the measure of stability (Figure 3). The results confirmed our hypothesis; with higher concentrations of platinum, a red shift of λ_{max} was observed (data not shown), corresponding with the overall AuNP charge approaching zero. A linear relationship exists between the concentration of cis-$\{Pt(NH_3)\}^{2+}$ added and zeta potential, a common measurement used to indicate stability,[34, 35] and is dependent upon nanoparticle size (Figure 3).

Aggregation and precipitation occurred at lower platinum concentrations for 55 and 90 nm AuNPs, and after precipitation zeta potential could not be measured. Using the zeta potential, and the observation of whether the nanoparticles remained in solution over time, we have determined the maximum amount of aquated cisplatin that can be used in the conjugation of platinum to the AuNPs, which will maintain nanoparticle stability: 25 nm, 0.94 $x10^{-12}$ molecules of platinum; 55 nm, 0.47 $x10^{-12}$ moles; and 90 nm, 0.19 $x10^{-12}$ moles.

Nanoparticle Characterisation

The different sized naked, PEGylated and drug-conjugated nanoparticles were analysed using a number of techniques to measure particle size, including: UV-visible spectrometry, atomic force microscopy (AFM) and DLS. UV-visible spectroscopy shows a red shift with increasing particle diameter with a λ_{max} around 518 nm for the 25 nm AuNPs, which is characteristic of gold nanoparticles around this size (Figure 4).[36] The 55 and 90 nm AuNPs have a λ_{max} around 528 and 563 nm, respectively.

To determine the particle size, the nanoparticles were analysed in the solid state using AFM (Figure 5). The naked AuNPs are roughly spherical in shape, particularly the 25 nm AuNPs, with the larger AuNPs showing improved shape distribution compared with previous nanoparticles of comparable size synthesised via the Turkevich-Frens method.[26] Their size correlates well with the results obtained by DLS, with the average diameter varying by less than 9%: 24.0 and 25.37 nm; 56.7 and 55.6 nm; and 97.3 and 89.2 nm (sizes determined by AFM and DLS, respectively). It should be noted that for the 90 nm AuNPs, we would expect the hydrodynamic diameter to be larger than that obtained from AFM.

The effect of PEGylation and drug conjugation on particle size was also determined by AFM and DLS (Figure 5). The AFM images indicate that there is no significant change in the size of the nanoparticles at any stage. Their hydrodynamic diameter in suspension, however, shows an increase in particle size upon PEGylation and drug conjugation. The naked 25 nm AuNPs demonstrate increases from 24.4 nm in size to 35.1 and 37.4 nm after PEGylation and platinum conjugation, respectively (Figure 5). The hydrodynamic diameter of the 55 nm AuNPs increases from 55.6 nm to 73.2 and 75.9 nm, and the 90 nm AuNPs from 89.2 nm to 107.2 and 106.0 nm upon PEGylation and conjugation, respectively. The increase in size after PEGylation can be used to determine the thickness of the PEG layer;[37] however any polydispersity in the size distribution makes this difficult.[38] The larger hydrodynamic diameters yielded by DLS for the latter two stages of assembly, compared to those observed for the naked AuNPs, are due to the interactions between the solvent and the covalently surface-bound PEG. This effect has been previously observed for PEGylated AuNPs,[39, 40] where hydrodynamic interactions are increased for large PEG linkers.[41] The polymer monolayer is decreasing the mobility of the nanoparticle,[42] most likely due to solvent interactions. The absence of aggregation when platinum is conjugated to the AuNP is an improvement on what we have previously published, where a 4.5-fold increase in size was observed in both the solution and solid state.[16] This is because, previously, the platinum drug used was the active component of oxaliplatin, {Pt(1*R*,2*R*-diaminocyclohexane)}, which has a cyclohexane-based ligand and may cause aggregation through hydrophobic self-interactions. Using the active component of cisplatin introduces polar ammine ligands which can hydrogen bond with water molecules and help retain stability in solution.

Determination of platinum content

The presence of platinum was confirmed by UV-visible spectrometry as spectra obtained were of a similar profile to previous studies of cisplatin in water, with a weak absorption band which can extend to 350 nm and a sharp increase in absorbance between 230 and 250 nm (Figure 6).[43] To quantitatively determine the number of platinum molecules per nanoparticle, the drug-nanoparticle conjugates were first digested using sodium cyanide,[44] and subsequently analysed by inductively coupled plasma mass spectrometry (ICP-MS). We have previously been able to demonstrate drug loading of up to 300 platinums per AuNP,[16] with another study showing up to 2,812 platinums per AuNP.[20]

In this study, the drug loading was found to increase significantly with increasing particle size: 25 nm (815 ± 106 drug molecules per AuNP); 55 nm (14,216 ± 880); and 90 nm (54,487 ± 15,996). The number of drug molecules conjugated to the AuNPs exhibit significant enhancement on all those previously published. This improved, high drug loading is important as it may lead to a significant increase in the dose delivered to tumours, especially in the case of the 90 nm drug-nanoparticle conjugates. If the cellular uptake and activity remains unaffected, the higher payload will result in increased cytotoxicity, and possibly even overcome some forms of drug resistance.

One issue, however, that must be resolved is the variability of the drug loading on the nanoparticles: 25 nm, 13%; 55 nm, 6%; and 90 nm, 29%.

Nanoparticle Stability

Nanoparticle instability may manifest as agglomeration and/or particle growth, both of which result in an increase in the diameter and a red shift of λ_{max} in the case of gold nanoparticles. Maintaining stability over time is essential for the efficacy and safety of AuNP-based drugs, as unstable nanosuspensions can affect administration and the dose delivered.[45]

A previous study which investigated the stability of 20 nm AuNPs synthesised via the Turkevich-Frens method, highlighted that nanoparticle growth and precipitation from solution is an issue.[46] When stored at room temperature, the nanoparticles grew up to 6.5-fold in size and at 4 ºC, although growth was less than when stored at higher temperature, the size of the nanoparticles increased to 40 nm.[46]

It was therefore of interest to study the stability of our AuNPs. We have used DLS to monitor changes in the hydrodynamic diameter of the nanoparticles over time, at room temperature and 4 ºC. We have examined naked and PEGylated nanoparticles and, for the first time, looked at the stability of platinum conjugated AuNPs. Compared with the previous study,[46] the 25 nm naked AuNPs demonstrate improved stability over a four week period, with an average maximum diameter of 33.2 and 26.3 nm when stored at room temperature and 4 ºC, respectively (Figure 7). The variation in size for the naked nanoparticles after 28 days was 2.4%. PEGylated and drug-conjugated AuNPs also show minimal variation in size at 4 ºC, with the average diameter after 28 days demonstrating only a 2.7 and 2.3% increase in size, respectively, from the initial measurement (Figure 7). When stored at room temperature, the 25 nm nanoparticles increase by 4.0 and 15.6% in size for the PEGylated and drug-conjugated nanoparticles. The growth of the nanoparticles is therefore dependent upon storage conditions and so, to maintain stability over time,

they should be stored at 4 ºC. The minimised growth at this temperature is postulated to be because at the higher temperature, there is more kinetic energy to encourage agglomeration, which results in larger particle sizes.[46]

As minimised growth was observed at 4 ºC for the 25 nm AuNPs, it was this temperature at which the stability of 55 and 90 nm AuNPs was examined. For either size, minimal growth is observed, regardless of whether the nanoparticles are naked, PEGylated or drug-conjugated (not shown). For the naked nanoparticles, the variation in average diameter after 28 days was 3.3 and 3.6%, for the 55 and 90 nm AuNPs, respectively. The results from the three different sized AuNPs show that the drug-conjugated nanoparticles exhibit enhanced stability compared with the previous two stages of assembly.

We also examined changes in UV-visible absorbance of the 25 nm AuNPs. This technique was used to assess AuNP stability as decreases in λ_{max} may have indicated that aggregation had occurred and/or the nanoparticles had precipitated. There were no drastic changes in absorbance, except for the PEGylated nanoparticles when stored at room temperature (Figure 7). The drop in concentration of the PEGylated AuNPs reinforces our earlier conclusion that gold nanoparticles should be stored at low temperatures.

This investigation has established that the method we have developed for AuNP synthesis produces naked nanoparticles which are relatively stable over time. We have also demonstrated that when stored at low temperatures, 25-, 55- and 90 nm-naked, PEGylated and drug-conjugated AuNPs exhibit a smaller degree of size variation over time.

Conclusions

For any new drug to get approval for human clinical trials, it must demonstrate not only efficiency, but also be able to be reproducibly manufactured and stored in a stable manner, whether the formulation is in solid form or an aqueous suspension. Previously we, and others, have shown that platinum drugs can be conjugated to AuNPs and that cellular uptake and cytotoxicity are significantly improved. To further develop AuNPs as platinum drug-delivery vehicles, it was essential to establish their level of reproducibly and stability. Here, we have reported a revised method for producing AuNPs that displays better size distribution and reproducibility for 25 nm AuNPs. For 55 and 90 nm AuNPs, the method shows improved nanoparticle shape and good reproducibility. Subsequent conjugation of the nanoparticles with the active component of cisplatin, cis-$\{Pt(NH_3)\}^{2+}$, showed enhanced drug loading, with the number of platinums per nanoparticle ranging from 700 to 70,000. An issue which must be addressed in the future, however, is the variability of the drug loading on each of the AuNP sizes. During drug conjugation, an increase in the concentration of cis-$\{Pt(NH_3)\}^{2+}$ led to an increase the overall charge of the nanoparticle, representative of the nanosuspension becoming unstable. Additionally, it has previously been shown that AuNPs can grow and/or aggregate when stored as suspensions. We have found that storage at 4 ºC and drug-conjugation of the nanoparticles improves their stability so they can be stored for several weeks without significant change. Overall, these results provide an important next step in the development of AuNPs as delivery vehicles for platinum drugs. To move forward, a large scale synthetic method should be developed so that AuNPs and their drug conjugates can be fully examined in vitro and in vivo.

Methods

Materials. All chemicals and solvents used were purchased from Sigma-Aldrich. All aqueous solutions were prepared using water filtered by a Millipore purification unit. The synthesis of aquated cisplatin followed a published method,[47] as did the synthesis of the polyethylene glycol (PEG) linker.[16]

Inductively coupled plasma – mass spectrometry. Before analysis, gold nanoparticles were digested into gold ions using a standard method of dissolution with sodium cyanide.[44] An Agilent 7700X instrument, with a micromist nebuliser and an octapole collision cell, was calibrated using solutions prepared from a Spex CertPrep platinum standard at concentrations ranging from 0 – 1000 ppb, containing 2% nitric acid. The platinum drug concentration on the AuNPs was determined using the ^{195}Pt isotope. Instrument operating conditions used were 1,550W RF forward power, 0.85 L min^{-1} plasma carrier gas flow, 0.2 L min^{-1} makeup gas flow, 4.6 mL min^{-1} helium gas flow in the collision cell and 0.1 rps for the nebulizer pump. Sample depth was 8 mm, sample period was 0.31 s and integration time was 0.1 s.

Dynamic light scattering. Dynamic light scattering and zeta potential experiments were conducted on a Malvern Zetasizer Nano ZS. The machine was calibrated using a 60 nm polystyrene standard. A 1 mL sample was loaded into a cell and the particle size and zeta potential were measured simultaneously 3 times with triplicate samples.

Atomic Force Microscopy. A gold nanoparticle suspension (5 µL) was deposited onto a freshly cleaved mica surface (G250-2 Mica sheets 2.54 cm x 2.54 cm x 0.015 cm; Agar Scientific Ltd, Essex, UK), and air dried for 30 min. The images were obtained by scanning the mica surface in air under ambient conditions using a Bruker

MultiMode with NanoScope IIID Controller Scanning Probe Microscope (Digital Instruments, Santa Barbara, CA, USA; Bruker software Version 6.14r1) operated in tapping mode. The AFM measurements were obtained using sharp silicon probes (TESP; nominal length (*lnom*) = 125 μm, width (*wnom*) = 40 μm, tip radius (*Rnom*) = 8 nm, resonant frequency (υ*nom*) = 320 kHz, spring constant (*knom*) = 42 N m^{-1} (Bruker Instruments SAS, Dourdan, France). AFM scans were taken at 512 x 512 pixels resolution and produced topographic images of the samples in which the brightness of features increases as a function of height. Typical scanning parameters were as follows: tapping frequency 322 kHz, integral and proportional gains 0.4 and 0.6, respectively, set point 0.4 – 0.6 V and scanning speed 1.0 Hz. AFM images were collected from two different samples and at random spot surface sampling (at least five areas).

Ultraviolet-visible spectroscopy. UV-visible spectra were obtained using a Varian Cary 50 Bio spectrophotometer running Cary WinUV scan software. Each sample (2 mL) was prepared at appropriate dilutions to achieve absorption values between 0 – 1. Samples were examined in a silica cuvette (1 cm) and an average of three measurements was used.

Synthesis of naked gold nanoparticles. All glassware used in the preparation of nanoparticles was soaked in aqua regia (3:1 HCl:HNO_3) for at least 4 h and then rinsed with distilled water until the water pH was neutral. $NaAuCl_4.2H_2O$ (50 mg, 0.14 mmol) was dissolved in a three neck round bottom flask using distilled water (500 mL). This was heated using a bunsen burner to 100 °C with continuous stirring by a double linked glass stirrer using a mechanical stirrer (Janke & Kunkel, Type RW20, speed setting “5.5”). Each neck of the flask was sealed with tinfoil to minimise loss of water by evaporation. Upon boiling, a fresh room temperature solution of

sodium citrate was added to achieve the desired size of nanoparticle (1% m/v stock solution: 25 nm, 20 mL; 55 nm, 3.7 mL; 90 nm, 2.1 mL). The solution was continuously boiled and stirred for 15 min before cooling to room temperature while stirring at a reduced speed (speed setting "2"). The colloid was concentrated by centrifuge (25 nm, 6000 rpm/2 h; 55 nm, 4000 rpm/ 20 min; 90 nm, 4000 rpm/10 min) and the supernatant liquid removed by decanting.

Assembly of platinum tethered nanoparticles. To an eppendorf vessel containing gold nanoparticles (1 mL: 25 nm, 17 nM; 55 nm, 0.17 nM; 90 nm, 0.017 nM), PEG linker was added (100 μL, 1 mM) and agitated for 4h by placing in a round bottom flask and spinning on a rotary evaporator. Unbound PEG linker was removed by centrifuging (7000 rpm: 25 nm, 20 min; 55 nm, 7 min; 90nm, 2 min), the supernatant liquid removed and the remaining pellet resuspended in water (1 mL). The washing process was repeated once more before *N,N*-diisopropylethylamine (100 μL, 0.1 mM) was added to the nanoparticles. This was followed by the addition of 25 μL of a *cis*-$[Pt(OH_2)_2(NH_3)_2]2NO_3$ dissolved in 1,3-dimethyl-3,4,5,6-tetrahydro-2(1*H*)-pyrimidone stock solution (25 nm, 10 mg/mL; 55 nm, 5 mg/mL; 90 nm, 2 mg/mL), and the nanoparticle left agitating overnight. Finally, the gold nanoparticles were centrifuged (same conditions as for the purification of PEGylated nanoparticles, Table 2), the supernatant liquid was removed and the remaining pellet resuspended in water (1 mL) before the wash was repeated once more.

References

(1) Kelland, L., *Nat. Rev. Cancer* **2007,** *7,* 573.

(2) Wheate, N. J.; Craig, G. E.; Walker, S.; Oun, R., *Dalton Trans.* **2010,** *39,* 8097.

(3) Matsumura, Y.; Maeda, H., *Cancer Res.* **1986,** *46,* 6387.

(4) Couvreur, P.; Dubernet, C.; Brigger, I., *Adv. Drug Delivery Rev.* **2002,** *54,* 631.

(5) Hobbs, S. K.; Monsky, W. L.; Yuan, F.; Roberts, W. G.; Griffith, L.; Torchilin, V. P.; Jain, R. K., *Proc. Nat. Acad. Sci. USA* **1998,** *95,* 4607.

(6) Perrault, S. D.; Walkey, C.; Jennings, T.; Fischer, H. C.; Chan, W. C. W., *Nano Lett.* **2009,** *9,* 1909.

(7) Turkevich, J.; Stevenson, P. C.; Hillier, J., *Discuss Faraday Soc.* **1951,** *11,* 55.

(8) Connor, E. E.; Mwamuka, J.; Gole, A.; Murphy, C. J.; Wyatt, M. D., *Small* **2005,** *1,* 325.

(9) Shukla, R.; Bansal, V.; Chaudhary, M.; Basu, A.; Bhonde, R. R.; Sastry, M., *Langmuir* **2005,** *21,* 10644.

(10) Jelveh, S.; Chithrani, D. B., *Cancers* **2011,** *3,* 1081.

(11) Lu, W.; Singh, A. K.; Khan, S. A.; Senapati, D.; Yu, H.; Ray, P. C., *J. Am. Chem. Soc.* **2010,** *132,* 18103.

(12) Senapati, D.; Singh, A. K.; Khan, S. A.; Senapati, T.; Ray, P. C., *Chem. Phys. Lett.* **2011,** *504,* 46.

(13) Wang, S.-H.; Lee, C.-W.; Wei, P.-K., *J. Nanobiotech.* **2010,** *8,* 1.

(14) Chithrani, B. D.; Ghazani, A. A.; Chan, W. C. W., *Nano Lett.* **2006,** *6,* 662.

(15) Jiang, W.; Kim, B. Y. S.; Rutka, J. T.; ChanWarren, C. W., *Nat. Nano* **2008,** *3,* 145.

(16) Brown, S. D.; Nativo, P.; Smith, J.-A.; Stirling, D.; Edwards, P. R.; Venugopal, B.; Flint, D. J.; Plumb, J. A.; Graham, D.; Wheate, N. J., *J. Am. Chem. Soc.* **2010,** *132,* 4678.

(17) Dhar, S.; Daniel, W.; Gijohann, D. A.; Mirkin, C. A.; Lippard, S. J., *J. Am. Chem. Soc.* **2009,** *131,* 14652.

(18) Min, Y.; Mao, C.; Xu, D.; Wang, J.; Liu, Y., *Chem. Comm.* **2010,** *46,* 8424.

(19) Ren, L.; Huang, X.-L.; Zhang, B.; Sun, L.-P.; Zhang, Q.-Q.; Tan, M.-C.; Chow, G.-M., *J. Mater. Biomed. Res. A* **2008,** *85,* 787.

(20) Xu, C.; Wang, B.; Sun, S., *J. Am. Chem. Soc* **2009,** *131,* 4216.

(21) Brust, M., Walker, M., Bethell. D., Schiffrin, D. J., Whyman. R., *J. Chem. Soc., Chem. Commun.* **1994,** 801.

(22) Kimling, J.; Maier, M.; Okenve, B.; Kotaidis, V.; Ballot, H.; Plech, A., *J. Phys. Chem. B* **2006,** *110,* 15700.

(23) Perrault, S. D.; Chan, W. C. W., *J. Am. Chem. Soc.* **2009,** *131,* 17042.

(24) Ji, X.; Song, X.; Li, J.; Bai, Y.; Yang, W.; Peng, X., *J. Am. Chem. Soc.* **2007,** *129,* 13939.

(25) Brown, K. R.; Daniel, G. W.; Natan, M. J., *Chem. Mater.* **2000,** *12,* 306.

(26) Frens, G., *Nat. Phys. Sci.* **1973,** *241,* 20.

(27) Ji, X.; Song, X.; Li, J.; Bai, Y.; Yang, W.; Peng, X., *Journal of the American Chemical Society* **2007,** *129,* 13939.

(28) Sutton, D.; Nasongkla, N.; Blanco, E.; Gao, J., *Pharm. Res.* **2007,** *24,* 1029.

(29) Kim, C.-K.; Ghosh, P.; Rotello, V. M., *Nanoscale* **2009,** *1,* 61.

(30) Reiter, W. J.; Pott, K. M.; Taylor, K. M. L.; Lin, W., *J. Am. Chem. Soc.* **2008,** *130,* 11584.

(31) Dougan, J. A., Karlsson, C., Smith, W. E., Graham, D., *Nucl. Acids Res.* **2007,** *35,* 3668.

(32) PersonalCommunication, *BBInternational* **2010,** *Gold nanoparticle extinction coefficients*.

(33) Famulok, M.; Mayer, G., *Nature* **2006,** *439,* 666.

(34) Chandran, P. R.; Naseer, M.; Udupa, N.; Sandhyarani, N., *Nanotechnology* **2012,** *23,* 015602.

(35) Ivanov, M. R.; Bednar, H. R.; Haes, A. J., *ACS Nano* **2009,** *3,* 386.

(36) Link, S.; El-Sayed, M. A., *J. Phys. Chem. B* **1999,** *103,* 4212.

(37) Xie, J.; Xu, C.; Kohler, N.; Hou, Y.; Sun, S., *Advanced Materials* **2007,** *19,* 3163.

(38) Budijono, S. J.; Russ, B.; Saad, W.; Adamson, D. H.; Prud'homme, R. K., *Colloids and Surfaces A: Physicochemical and Engineering Aspects* **2010,** *360,* 105.

(39) Cho, W.-S.; Cho, M.; Jeong, J.; Choi, M.; Cho, H.-Y.; Han, B. S.; Kim, S. H.; Kim, H. O.; Lim, Y. T.; Chung, B. H.; Jeong, J., *Tox. Appl. Pharmacol.* **2009,** *236,* 16.

(40) Mei, B. C.; Oh, E.; Susumu, K.; Farrell, D.; Mountziaris, T. J.; Mattoussi, H., *Langmuir* **2009,** *25,* 10604.

(41) Liu, Y.; Shipton, M. K.; Ryan, J.; Kaufman, E. D.; Franzen, S.; Feldheim, D. L., *Anal. Chem.* **2007,** *79,* 2221.

(42) Pons, T.; Uyeda, H. T.; Medintz, I. L.; Mattoussi, H., *J. Phys. Chem. B* **2006,** *110,* 20308.

(43) Lu, Q. B.; Kalantari, S.; Wang, C. R., *Mol. Pharm.* **2007,** *4,* 624.

(44) Gittins, D. I.; Caruso, F., *Advanced Materials* **2000,** *12,* 1947.

(45) Wu, L.; Zhang, J.; Watanabe, W., *Adv. Drug Delivery Rev.* **2011,** *63,* 456.

(46) Balasubramanian, S. K.; Yang, L.; Yung, L.-Y. L.; Ong, C.-N.; Ong, W.-Y.; Yu, L. E., *Biomat.* **2010,** *31,* 9023.

(47) Lippert, B., Platinum Nucleobase Chemistry. In *Progress in Inorganic Chemistry*, John Wiley & Sons, Inc.: 2007.

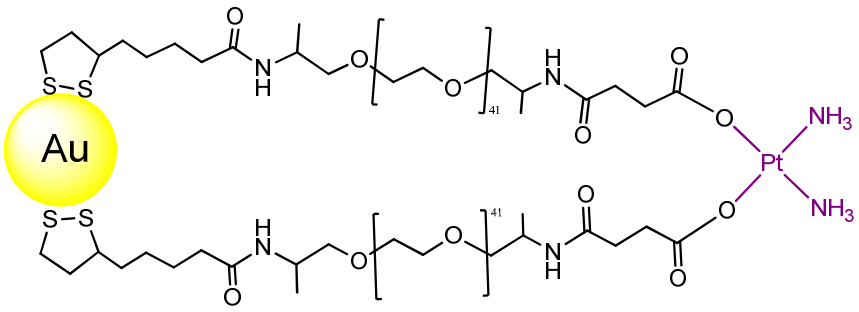

Figure 1. The drug-nanoparticle conjugate where the AuNP is functionalised with a polyethylene glycol (PEG) linker through a cyclic disulfide anchor and tethered to the active component of the anticancer drug cisplatin via the terminal carboxylate groups.

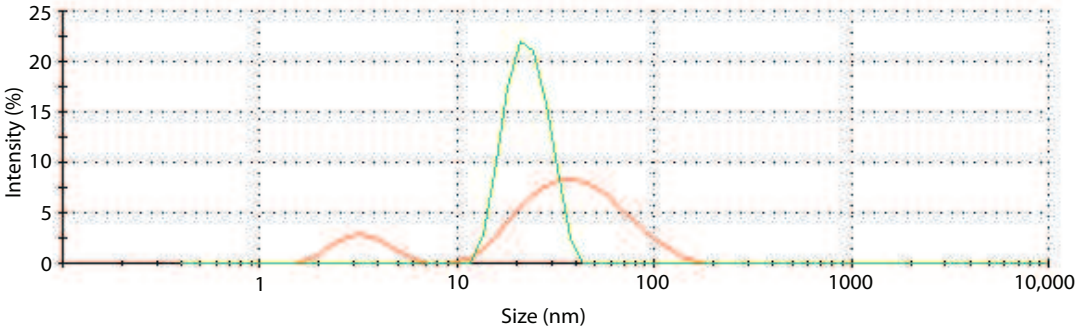

Figure 2. Dynamic light scattering spectra showing the diameter and distribution of 25 nm AuNPs synthesised via the established Turkevich-Frens method,[7, 26] (peaks at 3.4 and 45.4 nm) and our revised method, the latter showing monodispersity (peak average of 24.4 nm).

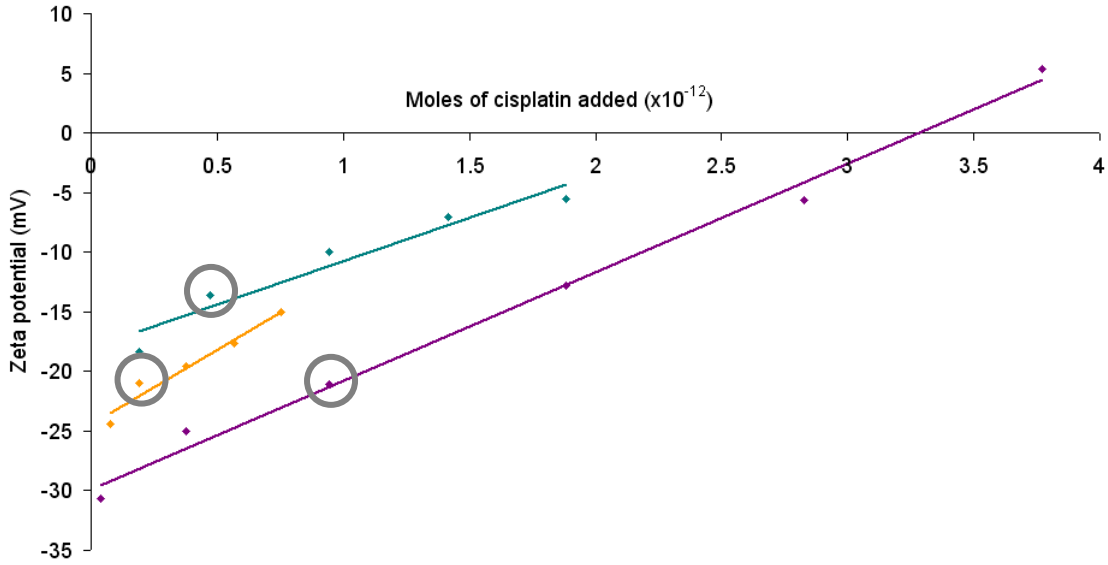

Figure 3. A graph showing the effect of platinum concentration on the charge of different sized AuNPs after drug conjugation: 25 nm (purple, r^2 = 0.9926); 55 nm (green, r^2 = 0.9318); and 90 nm (r^2 = 0.9567). For each size, the concentration of aquated cisplatin above which significant nanoparticle aggregation occurs is highlighted.

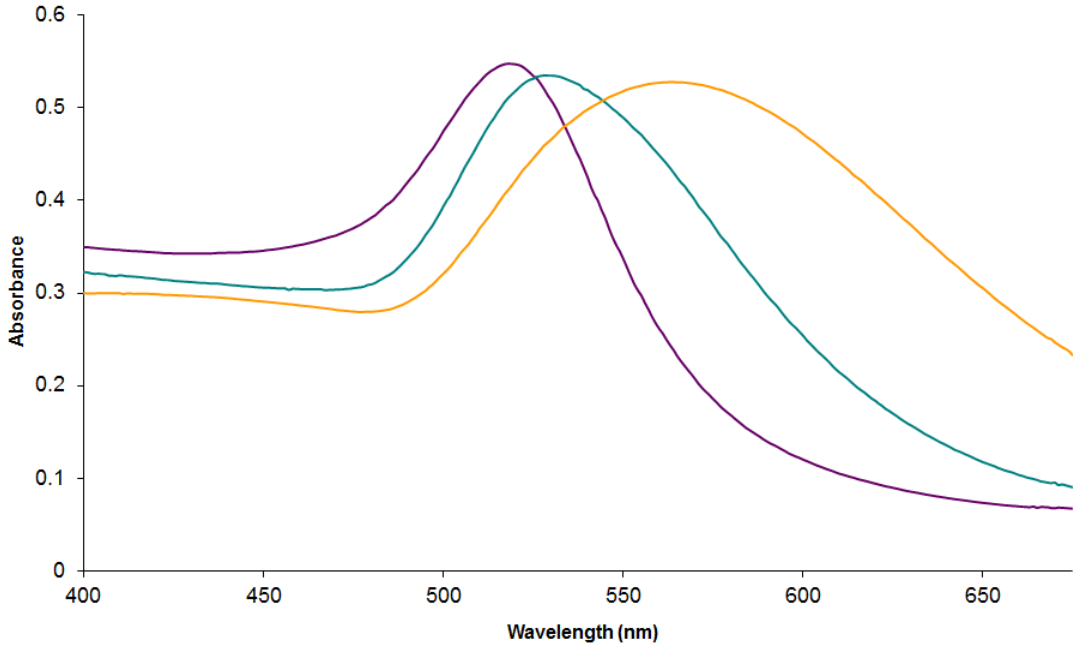

Figure 4. UV-visible spectra of the three different sized AuNPs: 25 nm (purple, λ_{max} = 518 nm); 55 nm (green, λ_{max} = 528 nm); and 90 nm (orange, λ_{max} = 563 nm), showing the expected red shift with increasing nanoparticle size.

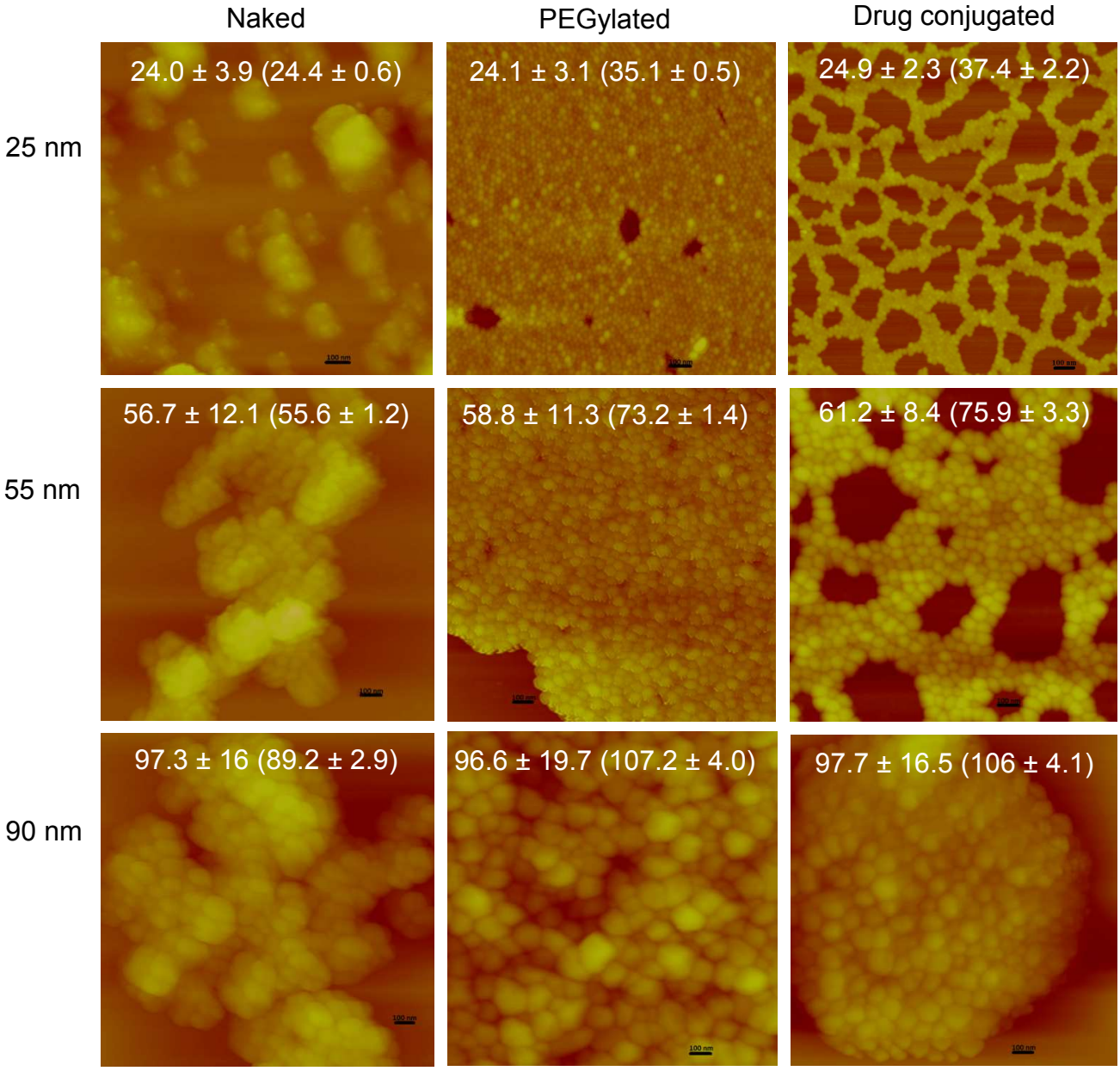

Figure 5. Atomic force microscopy images of the 25, 55 and 90 nm naked, PEGylated and drug conjugated AuNPs, showing the particle size as determined by AFM, and their hydrodynamic diameter (in brackets) obtained by DLS. An increase in the hydrodynamic diameter is observed upon PEGylation and platinum conjugation: 25nm, 44 and 52% (PEGylated and conjugated, respectively); 55nm, 32 and 37%; and 90 nm, 20 and 19%.

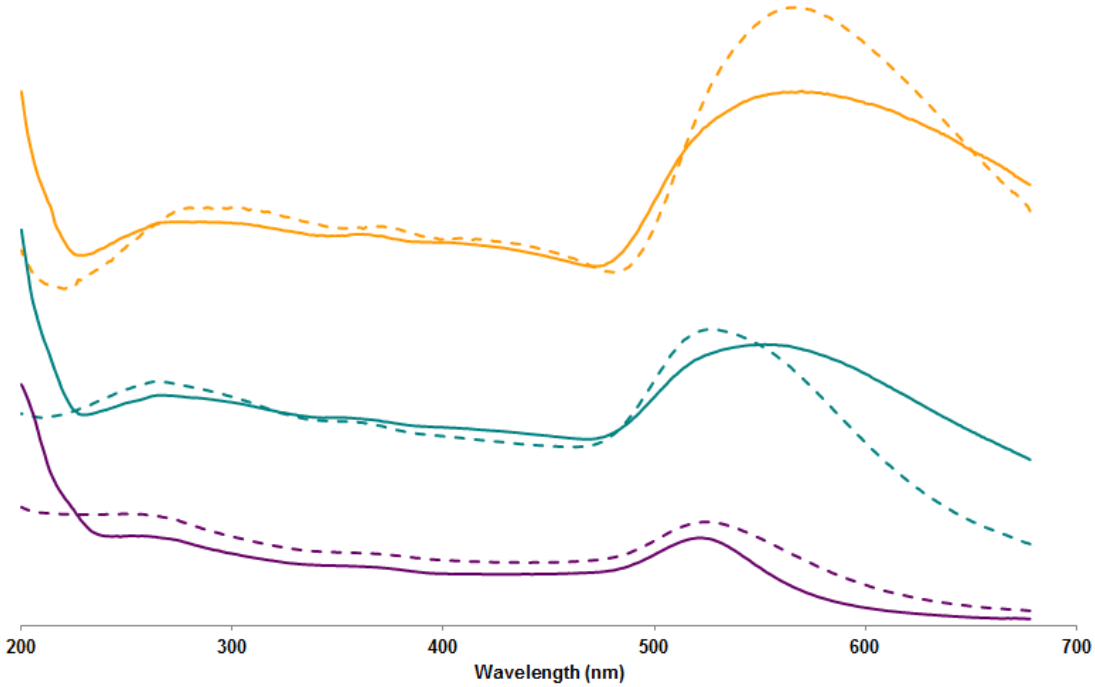

Figure 6. UV-visible spectra of PEGylated-only (dashed) and platinum-loaded (solid) AuNPs: 25 nm (purple), 55 nm (green) and 90 nm (orange). A red shift is observed compared with naked AuNPs (Figure 4) and on tethering the active component of cisplatin to the AuNPs, a sharp increase in absorbance is observed around 230 nm. Absorbance has been removed to stack spectra clearly.

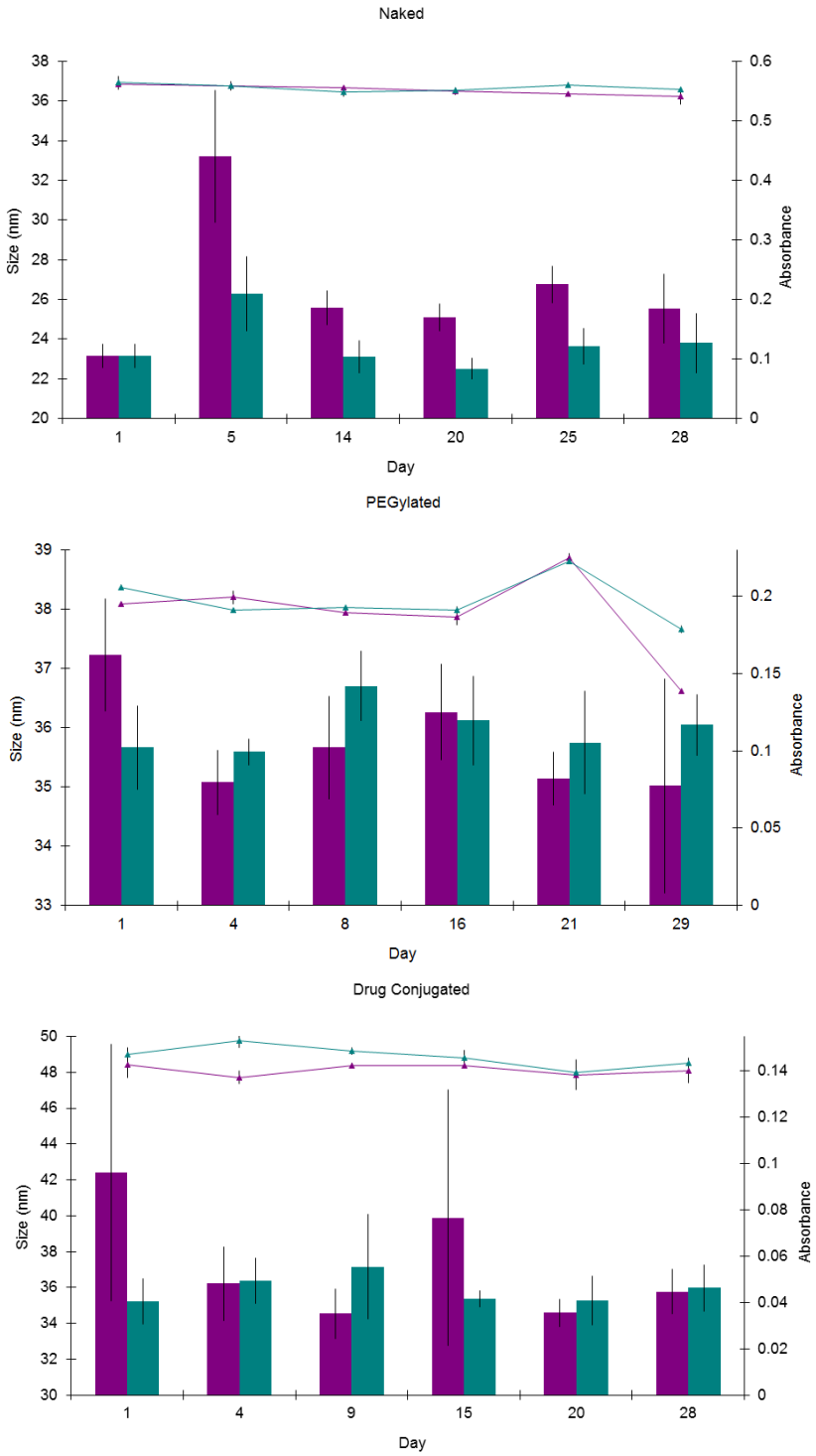

Figure 7. The stability of 25 nm AuNPs at each stage of assembly when stored at room temperature (purple) and at 4 ºC (green), with day 1 representing the day of synthesis. The bar chart represents the nanoparticle diameter in nanometres, as measured by DLS (left axis), and the line graph is nanoparticle absorbance, as measured by UV-Vis (right axis).

Table of contents graphic

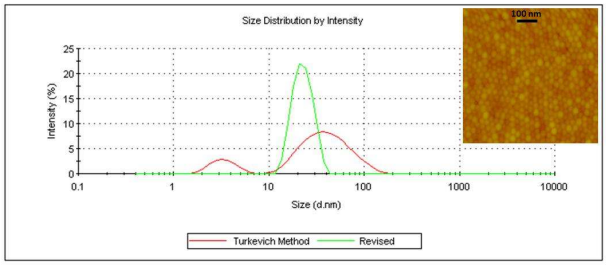

In this paper we have examined the synthesis, reproducibility, drug loading and stability of gold nanoparticles and analysed them as they relate to their use as delivery vehicles for platinum-based anticancer drugs.